

Surface Enhanced Raman Scattering Monitoring of Chain Alignment in Freely Suspended Nanomembranes

Chaoyang Jiang, Wilber Y. Lio, and Vladimir V. Tsukruk*

Department of Materials Science and Engineering, Iowa State University, Ames, Iowa 50011, USA

(Received 7 December 2004; published 9 September 2005)

The molecular chain reorganization in freely standing membranes with encapsulated gold nanoparticles was studied with surface enhanced Raman scattering (SERS) in the course of their elastic deformations. The efficient SERS was enabled by optimizing the design of gold nanoparticle forming chainlike aggregates, thus creating an exceptional ability to conduct *in situ* monitoring. Small deformations resulted in the radial orientation of side phenyl rings of polymer backbones while larger deflections led to the polymer chains bridging adjacent nanoparticles within one-dimensional aggregates.

DOI: 10.1103/PhysRevLett.95.115503

PACS numbers: 62.25.+g, 61.46.+w, 68.55.-a

The ultimate miniaturization of membrane-based sensor devices demands extremely robust membranes, while being sufficiently compliant enough to achieve record sensitivity, along with shrinking dimensions. Complex, freely standing nanostructures fabricated by the layer-by-layer (LBL) assembly can integrate various functional materials with nanoscale precision [1–4]. Such nanocomposites have already demonstrated extraordinary mechanical properties combined with high toughness [5]. These LBL nanomembranes have already demonstrated excellent sensing properties with an estimated limit of uncooled thermal detection below 1 mK, which is an order of magnitude better than ceramic cantilever-based assemblies [1]. The peculiar deformation behavior of their multilayered architecture was speculated to be responsible for the outstanding micromechanical properties [5,6]. However, the nature of the molecular mechanisms remains to be revealed.

To address this critical issue, a conformation sensitive spectroscopic technique, such as Raman spectroscopy, can be applied. It is known that stresses in bulk ceramic and metal matrices are widely analyzed with Raman spectroscopy [7–9]. However, for polymeric materials, a tremendous increase in signal intensity must be achieved to get structurally sensitive information. This becomes even more critical in the fast detection for materials with nanoscale thicknesses undergoing structural reorganization. Surface enhanced Raman scattering (SERS) generated by a curved metal surface (nanoparticles or nanocavities) must be applied in such cases [10,11]. SERS can tremendously enhance the signal for polymeric materials if properly designed metal surfaces are incorporated [12–14]. However, *real-time* monitoring of ongoing structural reorganizations from nanoscale materials (in femtogram amounts) is still a supreme technical challenge.

In this Letter, we report the *in situ* observation of molecular reorganization within nanocomposite (polymeric-metallic nanoparticles) LBL membranes in the course of their deformations by designing the optimal conditions for efficient SERS. The nanomembranes fabricated with spin-assisted LBL assembly are composed of a central

layer of gold nanoparticles (12.7 nm diameter) encapsulated within multilayered polymer walls (each wall with thickness around 20 nm) [Fig. 1(a)] [15,16]. The nanomembrane was freely suspended over openings with a diameter of 150 μm [Fig. 1(b)]. The concentration of gold nanoparticles confined within a two-dimensional inner layer was varied between 5% and 30% to achieve chainlike nanoparticle aggregation critical for the SERS enhancement [see inset in Fig. 1(b)]. The polymer walls were assembled from polyelectrolyte bilayers of poly(allylamine hydrochloride) (PAH, $M_w = 70000$) and poly(sodium 4-styrenesulfonate) (PSS, $M_w = 70000$) with the general formula $(\text{PAH-PSS})_n\text{PAH}/\text{Au}/(\text{PAH-PSS})_n\text{PAH}$, $n\text{Au}$, where n is the number of bilayers.

The behavior of nanomembranes has been studied on both a home-built interferometer and confocal Raman setup by applying pressure from one side and monitoring a corresponding membrane deflection from the resulting

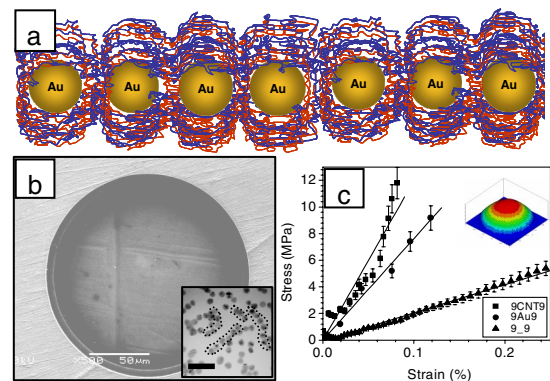


FIG. 1 (color online). (a) Microstructure of 9Au9 nanomembrane as suggested in Ref. [1]. (b) SEM image of the nanomembrane suspended over an opening in a copper plate; inset: TEM image of gold nanoparticle distribution into the nanomembrane, some chainlike aggregates are marked; bar: 40 nm. (c) Stress-strain plots derived from pressure-deflection data (solid lines show linear fits); inset: the deflected nanomembrane obtained from interferometry; the diameter is 150 μm .

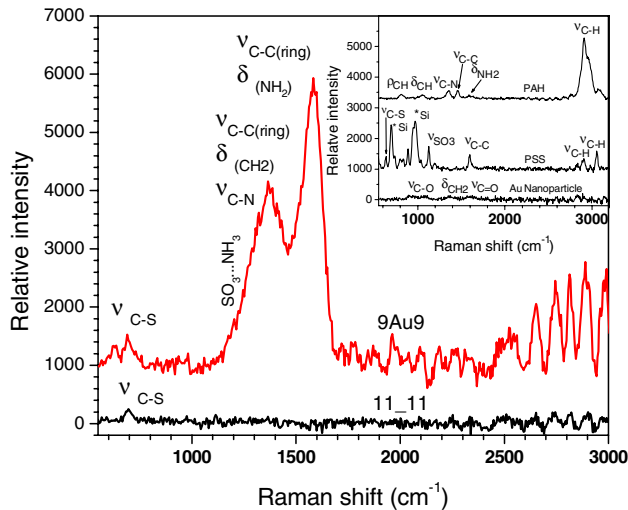


FIG. 2 (color online). Raman spectra of polymer and polymer-nanoparticles freely suspended nanomembranes in the rest state obtained under *identical* experimental conditions and showing dramatic enhancement of selected Raman bands. Inset: Raman spectra of bulk materials used for nanomembrane assemblies. The vibration modes are assigned according to the literature (ν , stretching; δ , bending; ρ , out-of-plane bending) (Table I).

formation of Newton's rings (interferometer) and SERS spectra (Raman spectrometer) [1]. A low laser intensity was used to avoid film damage (within 0.3–0.8 mW) and independent measurements showed the initial position of the main peak staying within ± 2 cm^{-1} with a broad variation of laser intensity (0.1–2 mW) and the peak positions remained identical to those obtained for the bulk polymers.

All nanomembranes studied here possessed nanoscale thickness within 35–60 nm and surface microroughness of 4–10 nm. Gold nanoparticles (3.9 vol. %) were randomly distributed as a central layer with a significant fraction forming chainlike aggregates composed of 6–10 nanoparticles with narrow (2–8 nm) gaps between neighboring

nanoparticles [inset of Fig. 1(b)]. The nanomembrane deflection under external pressure was converted into stress-strain data by using elastic plate theory [Fig. 1(c)] [1,17]. From near-linear stress-strain behavior found at low strains ($<0.2\%$), the elastic modulus of the 9Au9 nanomembrane was derived to be 5.7 ± 3.0 GPa as discussed elsewhere [18].

The Raman spectra obtained for bulk materials (cast films) displayed an excellent correspondence to the literature data with several strong peaks related to vibrations of different molecular groups as tabulated for identical and similar polymers in the literatures (Fig. 2, Table I). An assignment of the major sharp peaks of PSS according to the literature data for PSS and polystyrene (PS) materials included stretching vibrations at 2907 and 2831 cm^{-1} (C-H), 1589 cm^{-1} (phenyl ring in-plane C-C stretching), and 1035 and 1125 cm^{-1} (SO_3 and SO_2 stretching, respectively) [19,20,22,25]. The Raman spectrum for PAH showed strongest peaks with C-H stretching at 2908 cm^{-1} and bands at lower frequencies which have been associated in the literature with the stretching, bending, and wagging of the backbone groups [19,21,26]. Raman scattering from gold nanoparticles showed weak bands related to citric acid bonds (Fig. 2) [27].

In contrast, Raman scattering of free-suspended, purely polymeric nanomembranes was close to the instrumentation background without strong peaks (Fig. 2). Oscillations above 2500 cm^{-1} are spectral harmonics from the back-illuminated CCD camera, which are intensified by a strong background [28]. The only weak band observed at 696 cm^{-1} can be assigned to the C-S stretching of PSS chains. In fact, although the peak position differs from that reported in the literature for C-S stretching (761 and 670 cm^{-1}) [29], it is very close to 698 cm^{-1} position reported for antisymmetric C-S stretching for the compounds with C-S-O fragments which is more close to 1 studied here [24] and can be due to minor redistribution caused by the presence of oxygen [23].

The Raman scattering changed dramatically for the 9Au9 nanomembrane with encapsulated gold nanoparticles with chain-aggregated morphology. The overall intensity increased by several orders of magnitude and two strong dominating peaks became clearly visible (Fig. 2). The strongest peak around 1583 cm^{-1} is identical to that observed for bulk PSS for the in-plane C-C stretching of the side phenyl rings of PSS as assigned above (Table I) [19,20]. A strong peak was also observed for similar PSS:PAH LBL membranes [20]. The peak is wider (~ 90 cm^{-1}) than that usually observed for bulk materials, which can be due to contributions from PAH with slightly different positions (e.g., 1461 cm^{-1} for C-N bond) and the variable nanoparticle-polymer interactions as observed for LBL membranes [20]. A broad maximum between 1050 to 1400 cm^{-1} includes vibrations related to the bending and wagging of CH_2 groups, as well as stretching of the phenyl rings and C-N bonds according to literature data for similar polymers [26,30,31]. $\text{SO}_3 \cdots \text{NH}_3$ interactions which are a

TABLE I. Raman peak positions and corresponding assignments.

PAH, Bulk	PSS, Bulk	SERS PSS/PAH	Assignments	Position, Reference
3058	3053		$\nu\text{C-H}$,	3058, [19]
2908	2907		$\nu\text{C-H}$	2915, [19]
1594			δNH_2	1600, [20]
	1589	1583	$\nu\text{C-C}$ (ring)	1584, [19]; 1598, [20]
1457			$\nu\text{C-C}$ (ring), $\nu\text{C-N}$	1449, [19]; 1461, [21]
		1380	$\nu\text{C-C}$ (ring)	1367, [19]
	1125		νSO_2	1128, [20]
	1035		νSO_3	1037, [22]
1048			δCH	1061, [21]
	696	691	$\nu\text{C-S}$	697, [23]; 698, [24]

signature of these multilayers at 1200 cm^{-1} can also contribute to this maximum [20].

Finally, a peak observed at 691 cm^{-1} can be assigned to antisymmetric C-S stretching as discussed above with a slight redshift caused by interactions for gold surface. Additional weaker band at 628 cm^{-1} is more difficult to assign but considering the presence of the paired weaker symmetric band observed for C-S bond shifted by 31 cm^{-1} we can tentatively assign this peak to symmetric C-S stretching [23]. Larger redshift of this band in our membranes can be related to environment effect caused by the presence of gold surfaces and $\text{SO}_3 \cdots \text{NH}_3$ interactions. In fact, a significant redshift of this band (down to 612 cm^{-1}) was initiated by lower temperature and deuteration [24].

It is well known that the surface enhancement for selected vibrations indicates the preferential vertical orientation of the corresponding vibration and the proximity to the metal surface (within 1–4 nm) [10]. Considering that the estimated fraction of polymer chains confined between the gold nanoparticles is below 1%, we can evaluate the SERS enhancement factor to be 10^5 . Such high enhancement for the 1583 cm^{-1} peak and the absence of the peaks at 1000 cm^{-1} indicate that the side phenyl rings are oriented along the normal to the gold surface according to the literature data [32–35]. The enhancement of the peak at 1375 cm^{-1} , corresponding partially to C-N bonds from PAA side groups, confirms the close proximity of the PAH segments to the metal surface as well. Overall, this indicates an efficient intermixing of the PSS and PAH segments in the vicinity of the nanoparticles [5].

Because the optimal surface density of the nanoparticles within our nanomembrane (20%–25%) is well below the 2D percolation limit, and the nanoparticles form chainlike aggregates, most “hot spots” are localized within these chainlike aggregates providing the large enhancement unachievable otherwise. In fact, the narrow gap between the nanoparticles (2–8 nm) allows for several PSS-PAH chains (with a diameter of 0.5 nm) to be confined between neighboring nanoparticles promoting an efficient surface enhancement for polymer chains trapped [36–38]. The presence of strong SERS peaks caused by optimized one-dimensional aggregation of gold nanoparticles encapsulated between polymer multilayers allowed for *fast, real-time monitoring* of the internal structural reorganization of the free-suspended nanomembranes in the course of their elastic deflection, an unprecedented possibility.

The high-resolution SERS spectra from the 9Au9 nanomembranes were collected while pressing nanomembranes either to low (50–400 nm) or high ($0.4\text{--}7\text{ }\mu\text{m}$) deflections by applying up to 100 mbars from one side (Fig. 3). Two Raman peaks were analyzed using Lorentzian fitting to obtain their positions at different membrane deflections. Changes in relative peak intensity associated with group reorientation should be considered along with frequency shifts caused by delocalizations arising from an increase in the distance between the group and metal surface [39]. Despite significant scatter in the data due to the strong

background and different locations ($\pm 2\text{ cm}^{-1}$ for peak position and $\pm 30\%$ for the intensity ratio), the overall trend was reproducible and *reversible* (within $\pm 1\text{ cm}^{-1}$ for the peak position and $\pm 15\%$ for the intensity ratio for an individual set) with high temporary stability of all parameters.

The most important result obtained here is that *all variations* point to *nonmonotonic* internal reorganization with unexpected changes occurring at intermediate deflections. In fact, for small deformations (deflections below $2\text{ }\mu\text{m}$ or strain below 0.05%), the position of the main peak was gradually shifted to a higher frequency (from 1583 to 1589 cm^{-1}) while the position of the 1375 cm^{-1} peak shifted in the opposite direction, to 1368 cm^{-1} [Figs. 3(b) and 3(c)]. The trend changed to *the opposite* for the elastic deformation larger than $2\text{ }\mu\text{m}$ (a strain of 0.05%–0.6%): the main peak shifted 5 cm^{-1} to a lower frequency, and the secondary peak shifted to a higher frequency (1377 cm^{-1}) with the relative intensity I_{1585}/I_{1375} decreased by 50% (not shown). Considering the results obtained, we can conclude that the two-stage molecular reorganization occurs during microscopic deflections of free standing nanomembranes. This two-stage mechanism of the structural reorganization can be associated with two deformational regimes in continuum theory of elastic deformation of free-suspended plates. Bending deformation followed by in-plane tensile stretching [17].

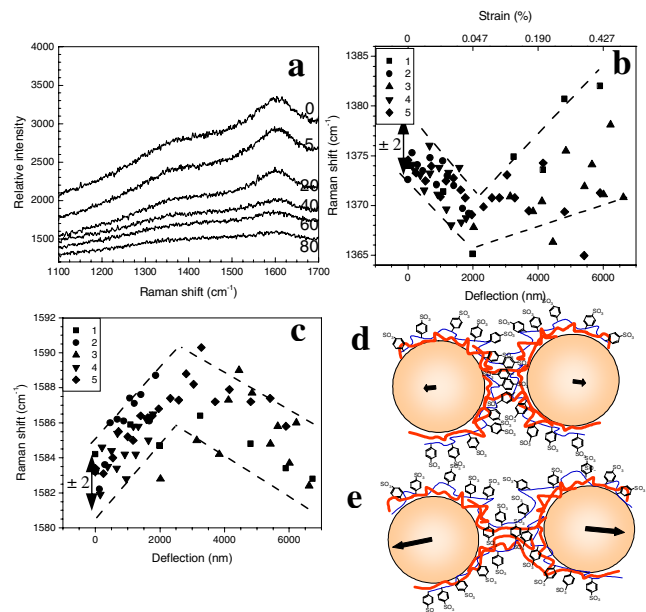


FIG. 3 (color online). (a) High-resolution SERS spectra obtained for free-suspended 9Au9 nanomembrane under increasing pressure (marked in mbars on the plot). (b), (c) The peak shift vs nanomembrane deflection for two peaks collected for five independent measurements from different locations (1–5); dashed lines show boundaries of variations of independent sets ($\pm 2\text{ cm}^{-1}$). (d), (e) Sketches of reorientation of side groups and backbone segments for low deformation (d) followed by the formation of bridging chain segments between gold nanoparticles for larger deformation (e).

For the membrane elastic behavior, we suggest that in a resting state, PSS/PAH backbones are spread close to the metal surface with a significant portion of the segments being in a planar orientation while the PSS side phenyl rings are oriented perpendicular to the nanoparticle surface [Fig. 3(d)]. The initial, small deformation of the elastic nanomembranes (below 0.05%) results in a slight increase of a gap within the one-dimensional, chainlike nanoparticle aggregates. This “gap widening” provides higher free volume which allows for the orientation of phenyl rings perpendicular to the backbone and, thus, in the radial direction in respect to the gold nanoparticles [Fig. 3(e)]. This segment realignment leads to the increasing intensity at 1583 cm^{-1} and the corresponding shift to a higher frequency. It is worth noting that long flexible chains (with an extended length up to 190 nm) could cover several neighboring nanoparticles, thus creating effective molecular bridging within the nanoparticle chain aggregates [Fig. 3(e)]. Therefore, further widening of the interparticle gap can no longer be accommodated without significant stretching of backbone segments in the radial direction. Their reorientation and the formation of the bridging segments lead to accompanying rearrangement of the side phenyl groups in the transversal direction, making them parallel to and increasing their distance from the metal surfaces. This reorganization inevitably makes the backbone segments orient perpendicular to and decouple from the metal surface.

In conclusion, the efficient SERS enabled by the optimized design of a gold nanoparticle inner layer encapsulated between polymer nanoscale walls (each about 20 nm thick) created an exceptional ability to conduct *in situ*, *real-time* monitoring of the internal reorganization of elastic nanomembranes in the course of their reversible elastic deformation. This unique experimental achievement revealed the *two-stage molecular mechanism* of the free-suspended LBL nanomembrane deformation in the form of the reorientation of the side groups followed by the stretching of the polymer backbone segments between neighboring nanoparticles. We suggest that such chain bridging of macromolecules spread, in the course of spin-assisted LBL assembly, over a number of adjacent gold nanoparticles within one-dimensional aggregates creates an effective toughening mechanism responsible for the outstanding robustness of these freely standing structures reported very recently [1,6].

The authors thank S. Markutsya and H. Shulha for assistance. This work is supported by AFOSR under Grants No. F496200210205 and No. F49620-03-1-0273.

*Author to whom correspondence should be addressed.

Electronic address: vladimir@iastate.edu

[1] C. Jiang *et al.*, *Nat. Mater.* **3**, 721 (2004).

- [2] A. Fery, F. Dubreuil, and H. Möhwald, *New J. Phys.* **6**, 18 (2004).
- [3] O.I. Vinogradova, *J. Phys. Condens. Matter* **16**, R1105 (2004).
- [4] *Multilayer Thin Films*, edited by G. Decher and J.B. Schlenoff (Wiley-VCH, Weinheim, 2003).
- [5] A.A. Mamedov *et al.*, *Nat. Mater.* **1**, 190 (2002).
- [6] C. Jiang *et al.*, *Appl. Phys. Lett.* **86**, 121912 (2005).
- [7] P. Colomban, *Adv. Eng. Mater.* **4**, 535 (2002).
- [8] S.K. Doorn *et al.*, *Phys. Rev. Lett.* **94**, 016802 (2005).
- [9] I. Loa, *J. Raman Spectrosc.* **34**, 611 (2003).
- [10] Z.-Q. Tian, B. Ren, and D.-Y. Wu, *J. Phys. Chem. B* **106**, 9470 (2002).
- [11] D.A. Genov *et al.*, *Nano Lett.* **4**, 153 (2004).
- [12] K. Kneipp *et al.*, *Phys. Rev. Lett.* **84**, 3470 (2000).
- [13] B. Pettinger *et al.*, *Phys. Rev. Lett.* **92**, 096101 (2004).
- [14] Y.C. Cao, R. Jin, and C.A. Mirkin, *Science* **297**, 1536 (2002).
- [15] C. Jiang, S. Markutsya, and V.V. Tsukruk, *Adv. Mater.* **16**, 157 (2004).
- [16] C. Jiang, S. Markutsya, and V.V. Tsukruk, *Langmuir* **20**, 882 (2004).
- [17] S. Timoshenko and S. Woinowsky-Krieger, *Theory of Plates and Shells* (McGraw-Hill, New York, 1959).
- [18] S. Markutsya, C. Jiang, Y. Pikus, and V.V. Tsukruk, *Adv. Funct. Mater.* **15**, 771 (2005).
- [19] W.M. Sears, J.L. Hunt, and J.R. Stevens, *J. Chem. Phys.* **75**, 1589 (1981).
- [20] W.-F. Dong, G.B. Sukhorukov, and H. Möhwald, *Phys. Chem. Chem. Phys.* **5**, 3003 (2003).
- [21] V. Zucolotto *et al.*, *J. Phys. Chem. B* **107**, 3733 (2003).
- [22] A. Kudelski, *Langmuir* **18**, 4741 (2002).
- [23] K.L. Kim, S.J. Lee, and K. Kim, *J. Phys. Chem. B* **108**, 9216 (2004).
- [24] W.N. Martens *et al.*, *J. Raman Spectrosc.* **33**, 84 (2002).
- [25] W.-F. Dong *et al.*, *Chem. Mater.* **17**, 2603 (2005).
- [26] G. Chumanov *et al.*, *J. Phys. Chem.* **99**, 9466 (1995).
- [27] T. Kemmitt *et al.*, *Inorg. Chem.* **43**, 6300 (2004).
- [28] K. Sokolov, G. Chumanov, and T.M. Cotton, *Anal. Chem.* **70**, 3898 (1998).
- [29] M. Larsson, J. Lu, and J. Lindgren, *J. Raman Spectrosc.* **35**, 826 (2004).
- [30] P.M. Secondo *et al.*, *Inorganica Chimica Acta* **309**, 13 (2000).
- [31] Y.-C. Liu *et al.*, *J. Phys. Chem. B* **108**, 14897 (2004).
- [32] S.-W. Joo and K. Kim, *J. Raman Spectrosc.* **35**, 549 (2004).
- [33] S.-W. Joo and Y.-S. Kim, *Colloids Surf. A* **234**, 117 (2004).
- [34] P. Leyton *et al.*, *J. Phys. Chem. B* **108**, 17484 (2004).
- [35] B. Pignataro *et al.*, *J. Chem. Phys.* **113**, 5947 (2000).
- [36] F. Festy, A. Demming, and D. Richards, *Ultramicroscopy* **100**, 437 (2004).
- [37] D.D. Evanoff, Jr., R.L. White, and G. Chumanov, *J. Phys. Chem. B* **108**, 1522 (2004).
- [38] K. Seal *et al.*, *Phys. Rev. B* **67**, 035318 (2003).
- [39] H.S. Kim *et al.*, *Langmuir* **19**, 6701 (2003).